2.7 Flow Reversals and Recirculation

Counterflows and closed circulations are commonly observed in experiments with hydraulically active rotating flows and have also been seen in deep passages such as the Hunter Channel (Zenk et al. 1999). Closed gyres tend to occur upstream of a controlling sill, typically along the northern hemisphere right wall, or downstream along the left wall. The later case occurs in connection with a hydraulic jump and will be discussed further in Chapter 3. Borenäs and Whitehead (1998) present examples of right-wall gyres, one of which is shown in Figure 2.7.1. The flow is confined to the lower layer of a two-fluid (water and kerosene) system in a rotating, rectangular channel vertical sidewalls. The channel is fitted with an obstacle that smoothly reaches a maximum height midway through the channel. The water is pumped into an upstream reservoir (to the left) where it collects and passes through a porous filter into the channel. The flow is critical at or very near the sill, the position of which is indicated by a dashed line. The gyre can be seen as a semicircular region of fluid that remains clear and free of dark dye introduced upstream.

The typical gyre geometry as seen in cross-section and plan view is sketched in Figure 2.7.2. The region of closed streamlines lies between two right-wall stagnation points at $y=y_1$ and $y=y_2$. The streamline joining the two points and located a distance w_g from the right wall will be called the stagnation streamline. The interface elevation along this contour must remain the same as that along the right wall, else the gyre would have a net geostrophic volume flux. The presence of a closed gyre gives rise to a number of questions concerning the physics and analysis of the flow. How is potential vorticity specified along the closed streamlines? Does the gyre choke the flow the same way that a contraction in channel width would? Before addressing these matters we first attempt to determine the conditions under which the right-wall gyre can form.

Counterflow is integral to the gyre and a mechanism that can work in favor of right-wall flow reversals is vortex squashing. As fluid columns leave a relatively deep reservoir and move towards a relatively shallow sill, their thickness d decreases and their vorticity $(\cong \partial v / \partial x)$ must decrease, perhaps becoming negative. This process can contribute to small or negative velocities along the right wall. Of course, the fact that counterflows are not observed in the downstream supercritical flow suggests that vortex squashing is not the whole story. Such flows tend to be separated from the left wall and therefore be much narrower than the upstream flow. Even though $\partial v / \partial x$ may be negative, the narrowness of the current and the strength of the (positive) mean velocity prevents v from becoming negative on the right wall.

A more careful examination of stagnation point formation and flow reversal may be made by appealing to earlier results on the formation of a counterflow. This subject was discussed in the context of a separated, zero potential vorticity flow, as summarized by the insets in Figure 2.3.2. Should this flow be critical at a sill, the interface will be level at the right wall (second inset from top) and v will vanish there. Immediately upstream from this section the flow will be subcritical (second inset from bottom), with

counterflow (v<0) along the right wall. In the laboratory example in figure 2.7.1, which is not separated, the counterflow begins a finite distance upstream of the sill.

The presence of a second, upstream stagnation point will terminate the counterflow and give rise to a closed gyre, as in the experiment. The existence of the second stagnation point may be anticipated using the expression for the right-wall velocity (2.2.4) based on uniform potential vorticity. If (2.2.18) is used this velocity may be expressed as

$$v(w/2,y) = q^{1/2}T\left[\frac{Q}{2\bar{d}T^2} + \bar{d} - q^{-1}\right], \qquad (2.7.1)$$

A right-wall stagnation point occurs where

$$\frac{Q}{2\bar{d}T^2} + \bar{d} - q^{-1} = 0,$$

or

$$\bar{d} = \frac{q^{-1}}{2} \pm \sqrt{\frac{q^{-2}}{4} - \frac{Q}{2T^2}} \quad . \qquad (2.7.2)$$

Two stagnation points are possible for $Q < T^2 q^{-2}/2$ and both will be encountered if $\bar{d}$ passes through the two indicated roots. This situation is favored by weak transports (Q<<1), small values of the potential vorticity (q<<1), or wide channels (T=$tanh[q^{1/2}w/2]$≅1). In addition, strong shoaling of the bottom encourages a greater range of $\bar{d}$ along the channel, and this increases the probability that two stagnation points will occur.

Can a counterflow exist at a control section? Under conditions of uniform potential vorticity and rectangular cross section this possibility is ruled out by the theorem constraining critical flow to be unidirectional (Section 2.5, Exercise 1). However, this restriction does not generally hold. We will identify examples showing that counterflows can occur at a critical section when the geometry is nonrectangular (Section 2.8) or when the potential vorticity is non-uniform (Section 2.9).

In dynamical terms, one of the distinguishing characteristics of a closed gyre is that the potential vorticity distribution is no longer imposed by upstream conditions. Fluid parcels are free to circulate indefinitely and dissipative effects, while arguably negligible for the throughflow, become paramount. An instructive constraint may be written down by integrating the tangential component of (2.1.15) around the circuit Γ_ψ formed by any closed streamline ψ=constant within the gyre. For steady flow, the result is

$$\oint_{\Gamma_\psi} \mathbf{F}^* \cdot \mathbf{l} ds = 0 \,, \qquad (2.7.3)$$

where $\mathbf{l}$ and ds are tangential unit vectors and differential arc length along Γ_ψ. The vector $\mathbf{F}^*$, which generally contains all momentum forcing and dissipation terms, might in the present context consist of a bottom drag term of the form $C_d \mathbf{u} / d$ (consistent with an Ekman layer on the bottom) and a lateral stress term $\boldsymbol{S}$. In the laminar laboratory flow (Figure 2.6.1) $\boldsymbol{S}$ is presumably dominated by the lateral viscous stress generated by the throughflow moving along the left side of the gyre and the wall on the right. In geophysical applications the lateral stress would be dominated by turbulent momentum fluxes. One of the difficulties in using (2.7.3) to solve for the circulation is that the shape of the latter is generally not known in advance. The immediate importance of (2.7.3) is that forcing and dissipation cannot be ignored once the streamlines are closed.

In order to incorporate a gyre into a hydraulic model for the flow as a whole, it is necessary to know something about the potential vorticity distribution along the closed streamlines. Borenäs and Whitehead (1998) explored two approaches, the first based on the assumption that the gyre potential vorticity has the same (constant) value as the throughflow and the second that the gyre is stagnant. The first approach has the virtue of simplicity; solutions may be calculated from the relations laid out in the Gill model (Section 2.5). The second approach is more consistent with observations of the laboratory flow, which show the gyre circulation to be relatively weak. The novel features of the calculation are explored in Exercise 1. Neither approach is easily motivated by dynamical principles. Determination of the true distribution of potential vorticity within the gyre remains an unresolved issue.

A comparison between gyres with uniform potential vorticity and stagnant fluid, both with the same upstream conditions, appears in Figure 2.7.3. The former is distinguished mainly by its strong anticyclonic circulation. Note that the positions of the stagnation points for the two cases are identical, as they must be (Exercise 2). The overall shape and size are similar. The gyre length tends to be moderately shorter than what is observed in the laboratory (Figure 2.7.4). The observed gyre widths (not shown in the figure) are also somewhat smaller than those predicted by either theory. A possible reason for the discrepancy is that the observed gyres often contained small cyclonic features. The experiment agrees with the theoretical prediction of a minimum width below which no gyre forms, though the threshold values are somewhat different.

Since a closed gyre carries no net volume transport, there is a temptation to think of the gyre edge as being equivalent to a solid wall. If the flow is steady and lateral viscous effects are ignored, the throughflow is apparently unaffected by replacing the stagnation streamline $x=(w/2)-w_g$ by a such a wall. In this view, the gyre might choke the flow in same way as a true side wall contraction. One must be wary of this analogy: if the stagnations streamline is replaced by a wall, the value of $T=tanh[q^{1/2}w/2]$ is replaced by $T=tanh[q^{1/2}\,(w-w_g)]$, and the value of the corresponding Froude number (2.5.7) is altered. The value based on placing an artificial wall at $x=(w/2)-w_g$ is invalid since it does not

account for the true physical characteristics of a Kelvin wave propagating through the flow. Such a wave would see the gyre edge as pliant, and not a rigid wall.

Exercises

1. Suppose that the gyre is stagnant and that the exterior fluid (the throughflow) has uniform potential vorticity (as in Figure 2.6.3b). What is the matching condition along the separating streamline that allows solutions in the two regions to be joined?

2. Show that the positions y_1 and y_2 of the stagnation points are independent of the potential vorticity distributions inside the gyre, provide that the potential vorticity of the exterior (non-circulating) fluid is the same constant.

Figure Captions

2.7.1 A gyre in a channel flow with a parabolic sill (from Borenäs and Whitehead, 1998). The left-to-right flow is marked by dark dye, which is introduced at the upstream end of the channel and is deflected around the gyre. The value of $wf/2\sqrt{g'D_\infty}$ is varied between 0.25 and 0.39, and the case shown has value 0.35. The velocity of the flow entering the left end of the channel has been rendered approximately uniform by a filter. The potential vorticity is therefore not uniform.

2.7.2 Diagram showing the recirculation and throughflow in cross section (top) and in plan view (bottom).

2.7.3 Comparison between gyres imbedded in the throughflow with uniform potential vorticity. The gyre can have the same uniform potential vortiticy as the throughflow (left) or be stagnant (right). Each case is characterized by $w^* f / (2gD_\infty)^{1/2} = 0.39$. From Borenäs and Whitehead (1998).

2.7.4 The gyre length as measured by the dimensionless distance between stagnation points $Y = (y_2 - y_1) f / [2(gD_\infty)^{1/2}]$ and plotted as a function of the dimensionless width $w^* f / [2(gD_\infty)^{1/2}]$. The curve is based on a theory with uniform potential vorticity upstream flow with $\psi_i = 1$ and with the experimental values $q = 0.25$ and $h^*_m / D_\infty = 3/4$.

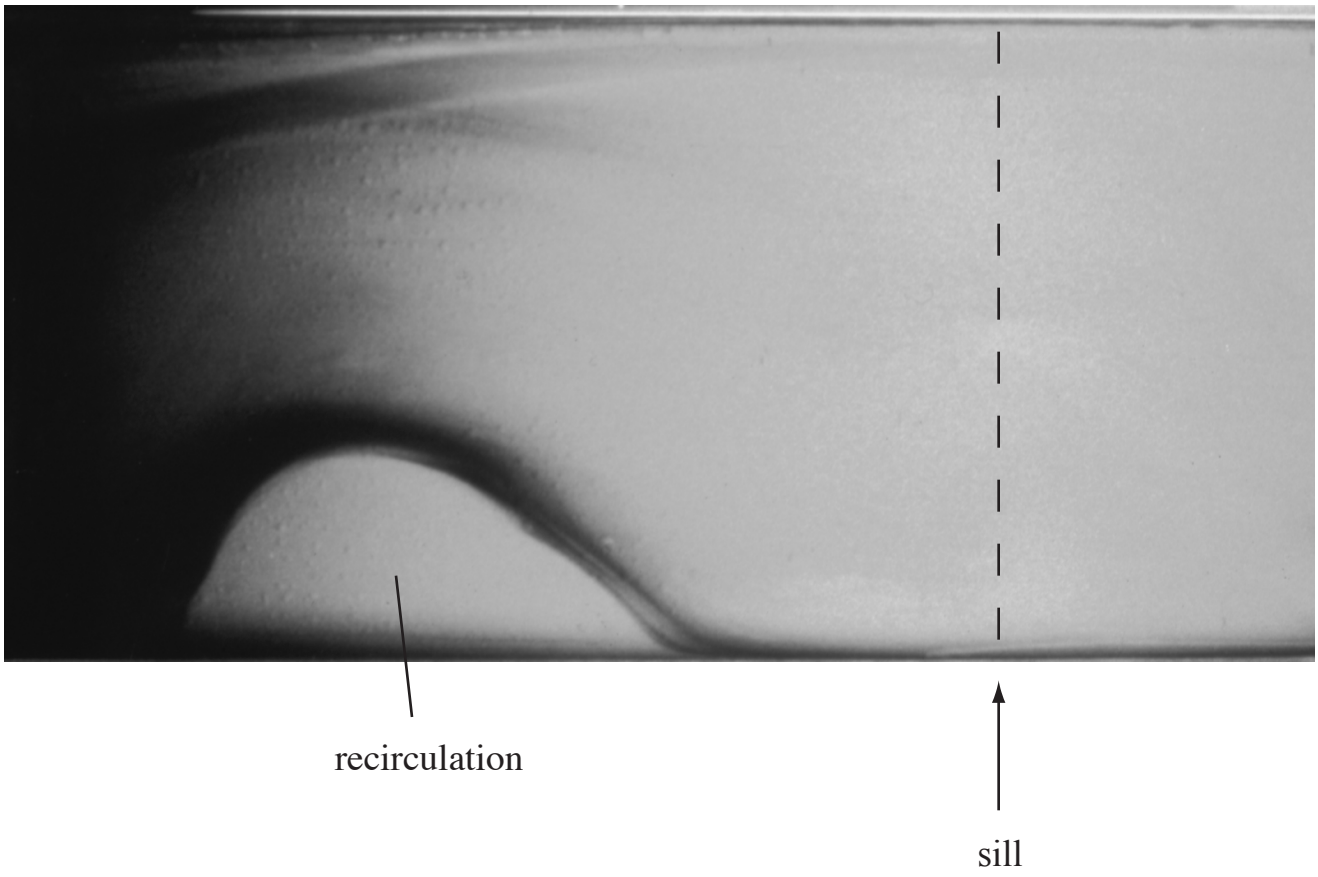

Figure 2.7.1

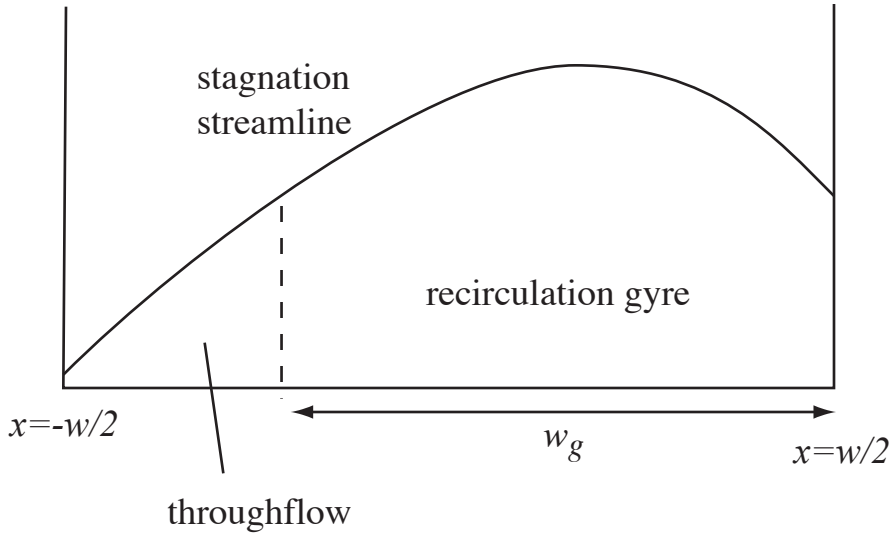

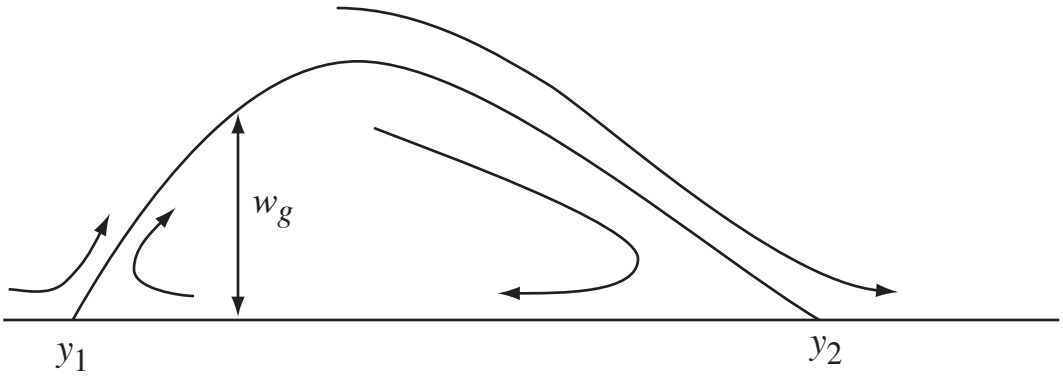

stagnation
point

stagnation
point

Figure 2.7.2

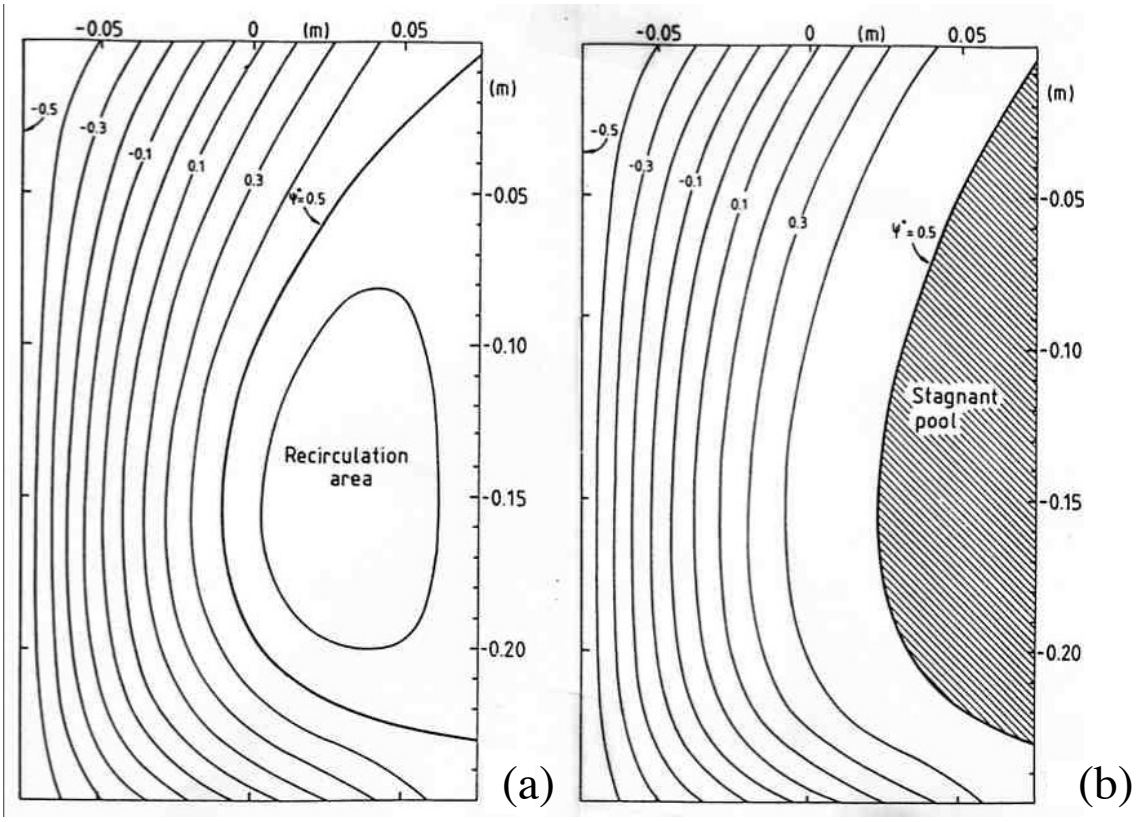
-0.05
0
(m)
0.05
-0.5
-0.3
-0.1
0.1
0.3
ψ*=0.5
(m)
-0.05
-0.10
-0.15
-0.20
Recirculation area
(a)
-0.05
0
(m)
0.05
-0.5
-0.3
-0.1
0.1
0.3
ψ*=0.5
(m)
-0.05
-0.10
-0.15
-0.20
Stagnant pool
(b)

Figure 2.7.3

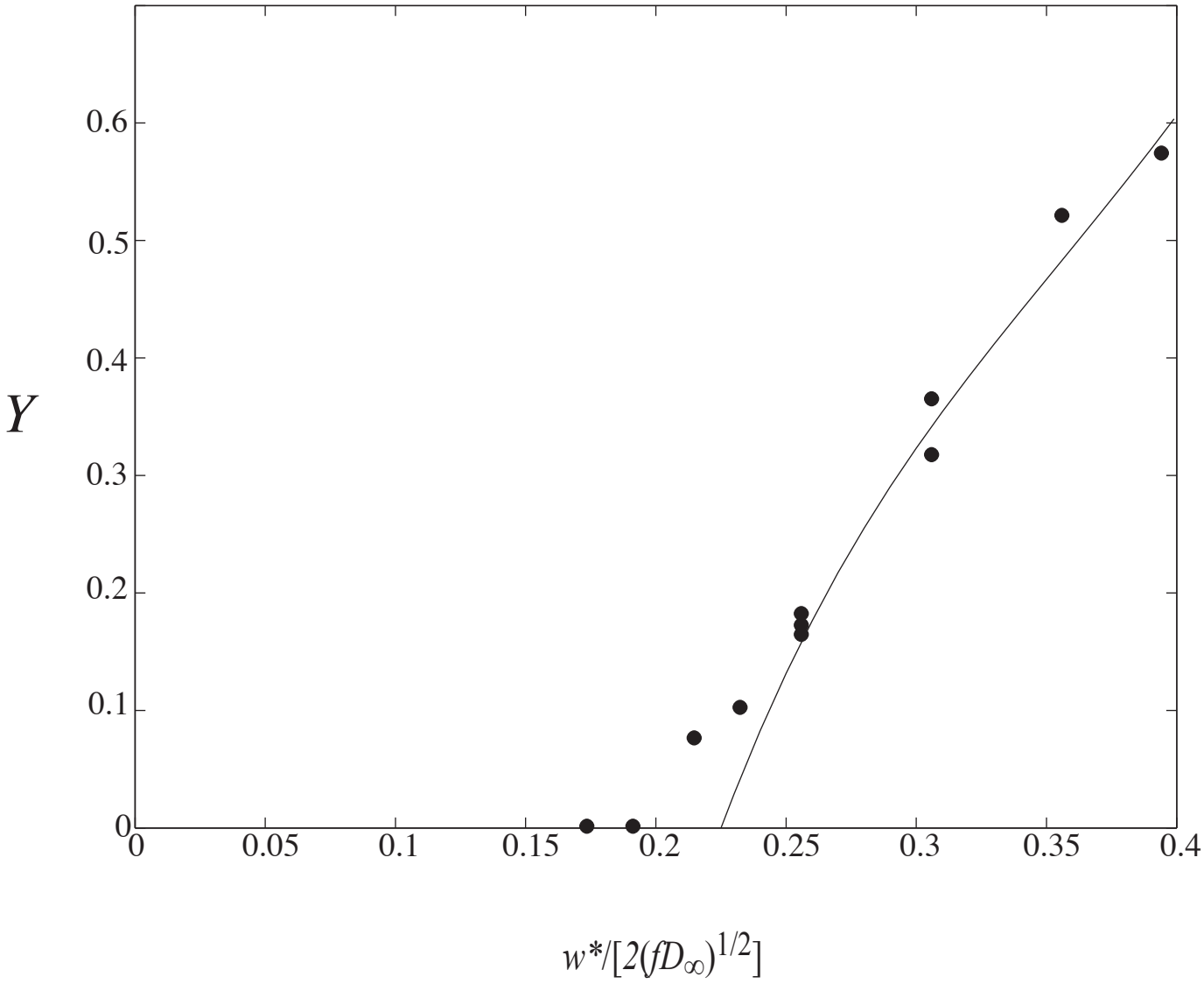

Figure 2.7.4